Contents lists available at ScienceDirect

Chemical Engineering Research and Design

journal homepage: www.elsevier.com/locate/cherd

Investigation of the radial effect on the transition velocities in a bubble column based on the modified Shannon entropy

Stoyan Nedeltchev[a,*], *Uwe Hampel*[a,b], *Markus Schubert*[a]

[a] *Helmholtz-Zentrum Dresden-Rossendorf, Bautzner Landstrasse 400, 01328 Dresden, Germany*
[b] *AREVA Endowed Chair of Imaging Technologies in Energy and Process Engineering, Dresden University of Technology, Germany*

ARTICLE INFO

Article history:
Received 8 April 2016
Received in revised form 26 July 2016
Accepted 8 August 2016
Available online 16 August 2016

Keywords:
Bubble column
Gas holdup fluctuations
Wire-mesh sensor
Transition velocities
Shannon entropy ratio

ABSTRACT

A new parameter for flow regime identification in a bubble column based on the calculation of the Shannon entropy (SE) from different parts of the signal was developed. The bubble column (0.15 m in ID) was equipped with a perforated plate distributor (14 holes, Ø 4×10^{-3} m) and operated with an air-deionized water system at ambient conditions. The newly introduced dimensionless ratio of minimum SE to maximum SE was capable of identifying the main transition velocities U_{trans} at three different dimensionless radial positions (r/R): 0.0 (core), 0.63 (inversion point of axial liquid velocity) and 0.88 (annulus).

In the column's core the new dimensionless SE ratio identified successfully three U_{trans} values at 0.034, 0.089 and 0.134 m/s. They marked the end of the gas maldistribution regime, the onset and the end of the churn-turbulent flow regime, respectively. Three U_{trans} values (at 0.045, 0.089 and 0.124 m/s) were also identified in the annulus. However, the second U_{trans} value identified the boundary between the first and second transition sub-regimes. The third U_{trans} value distinguished the onset of the churn-turbulent flow regime. It was found that in the core both the transition and churn-turbulent flow regimes started earlier.

At $r/R = 0.63$ the end of the gas maldistribution regime was shifted to a somewhat higher U_{trans} value (0.067 m/s). The second transition sub-regime began at 0.101 m/s, whereas the onset of the churn-turbulent regime occurred at 0.124 m/s.

1. Introduction

Bubble columns are characterized by an effective phase contact, high mass and heat transfer coefficients, low maintenance and operating costs due to the absence of moving parts, high catalyst life time and low column pressure drop (Kantarci et al., 2005). Due to their numerous advantages bubble columns are extensively used in many applications and processes such as oxidation, hydrogeneration, chlorination, waste water treatment and Fischer-Tropsch synthesis. Therefore, it is essential to have detailed knowledge about the hydrodynamic features of these gas–liquid contactors.

The study of the flow regime transitions in bubble columns is important for improvement of their design, operation and control. Since the degrees of mixing, mass and heat transfer are strongly affected by the prevailing flow regime, it is essential to develop reliable methods for a successful identification of its boundaries.

In bubble columns operating at ambient conditions three main hydrodynamic regimes are usually observed. At superfi-

* *Corresponding author.*
E-mail addresses: s.nedeltchev@hzdr.de (S. Nedeltchev), m.schubert@hzdr.de (M. Schubert).
http://dx.doi.org/10.1016/j.cherd.2016.08.011

Nomenclature

KE	Kolmogorov entropy (bits/s)
N	Number of data points (–)
$p(x)$	Probability that a certain value will appear in a specific part of the signal (–)
r/R	Dimensionless radius (–)
SE	Shannon entropy (nats)
SE_{FH}	Summed Shannon entropy in the first half of time series (nats)
SE_{max}	Maximum Shannon entropy (nats)
SE_{min}	Minimum Shannon entropy (nats)
SE_{SH}	Summed Shannon entropy in the second half of time series (nats)
U_G	Superficial gas velocity (m/s)
U_{trans}	Transition gas velocity (m/s)
x_i	Point i in the time series (%)

cial gas velocities U_G lower than 0.04 m/s, the homogeneous (or bubbly) flow regime is observed, which is characterized by relatively small bubbles of narrow size distribution. The gas–liquid dispersion is only gently agitated and a uniform gas holdup profile is observed. The gas distributor strongly affects the flow structure (pattern) in the bubble bed and coalescence events are insignificant.

The transition from the homogeneous to the heterogeneous (or churn-turbulent) flow regime is a gradual process. In between these two main hydrodynamic regimes a transition flow is observed. It is characterized by a widened bubble size distribution and local liquid circulation patterns.

The churn-turbulent flow regime, in turn, is characterized by the formation of larger bubbles whose wakes cause gross circulation patterns. There is a large bubble size distribution and a pronounced radial gas holdup profile. In this flow regime, the bubble bed is characterized by vigorous mixing and significant bubble coalescence. The gas distributor has only a little effect on the entire bubble column hydrodynamics.

The boundaries of the three main hydrodynamic regimes are delineated by two transition velocities U_{trans}: the first one distinguishes the boundary between homogeneous and transition flow regime, whereas the second one distinguishes the boundary between transition and churn-turbulent flow for appearance. The first U_{trans} value is more important, since it takes part in the calculation of both large bubble diameter and large gas holdup (Krishna and Ellenberger, 1996). Two correlations for the prediction of the first U_{trans} value in bubble columns have been reported in the literature. The one proposed by Reilly et al. (1994) is considered to be much more reliable than the correlation of Wilkinson et al. (1992).

The first flow regime map has been published by Shah et al. (1982). Since then, numerous new methods have been developed and new experimental results have been published in the literature (see Table 1).

It is worth mentioning that most of the research work on this subject has been performed with air-water system. The value of the first transition velocity can be predicted reliably based on the correlation of Reilly et al. (1994) which takes into account the physicochemical properties of both phases. However, there is no any theoretical or empirical correlation for the prediction of the second transition velocity. For this purpose, reliable new methods for flow regime identification have been developed recently by Nedeltchev and coworkers (2013, 2015, 2016). Especially, the reconstruction entropy (Nedeltchev, 2015) is considered as a very powerful method for a reliable identification of both main transition velocities based on well-pronounced local minima.

Table 1 – Summary of the main publications on flow regime identification in bubble columns based on different experimental techniques and methods of analysis.

Publication	Method used
Anderson and Quinn (1970)	Visual observation
Maruyama et al. (1981)	Visual observation
Reilly et al. (1994)	Gas holdup measurements
Kikuchi et al. (1997)	Nonlinear chaos analysis
Letzel et al. (1997)	Nonlinear chaos analysis
Lin et al. (1999)	Gas holdup measurements
Vial et al. (2000, 2001)	Analysis of pressure fluctuations
Lin et al. (2001a,b)	Nonlinear chaos analysis
Olmos et al. (2003a)	Analysis of laser Doppler anemometry signals
Olmos et al. (2003b)	Numerical description of flow regime transitions
Monahan et al. (2005)	CFD predictions for flow regime transitions
Ajbar et al. (2009)	Nonlinear chaos analysis
Shiea et al. (2013)	Analysis of resistivity probe signals
Nedeltchev et al. (2003, 2006, 2007, 2011), Nedeltchev and Shaikh (2013), Nedeltchev (2015)	Nonlinear chaos analysis
Nedeltchev et al. (2015), Nedeltchev (2015)	Information entropy theory

In the past two decades, several interesting papers on the flow regime transition in bubble columns have been published. Zahradnik et al. (1997) published an interesting paper about the duality of the flow regimes in bubble columns. Ruzicka et al. (2001a) studied the effect of bubble dimensions on the flow regime transition. Ruzicka et al. (2001b) focused their research on the homogeneous-to-heterogeneous regime transition in bubble columns. Later, Ruzicka et al. (2003) investigated the effect of liquid viscosity on homogeneous-to-heterogeneous flow regime transition in bubble columns. Ribeiro and Mewes (2007) studied the influence of electrolytes on the first transition velocity. Shaikh and Al-Dahhan (2007) reviewed exhaustively the literature on flow regime identification in bubble columns. Rabha et al. (2014) performed a comparative study on the regime transition in viscous and pseudo viscous systems. Pourtousi et al. (2014) studied the effect of interfacial forces and turbulence models on predicting the flow pattern inside the bubble column. Besagni and Inzoli (2016) studied the flow regime transition in counter-current bubble columns.

The main objective of this work is to investigate the effect of the radial position on the transition velocities in a bubble column. This dependency is so far fully ignored in the literature and to the best of the authors knowledge there is no any systematic study available. In order to investigate the radial effect, a new dimensionless parameter based on a modification of the Shannon entropy algorithm was used.

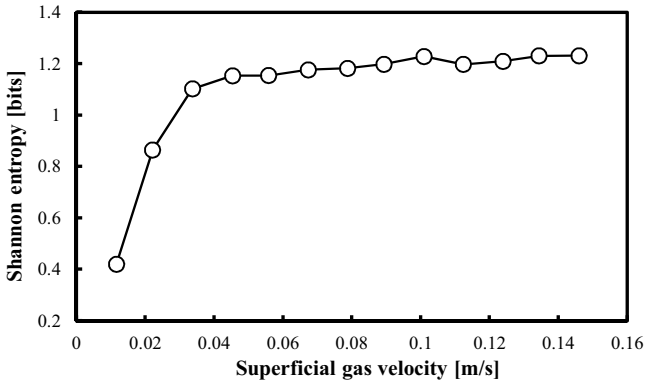

Fig. 1 – Profile of Shannon entropy as a function of U_G in the annulus ($r/R = 0.88$).

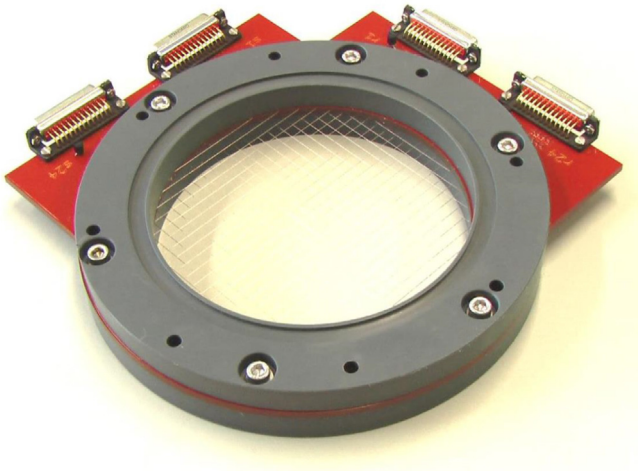

Fig. 2 – Photograph of the applied wire-mesh sensor.

2. Modified Shannon entropy

The Shannon entropy (SE) is a measure of the amount of information in a certain source (for example a time-dependent signal) and of the degree of indeterminacy in a certain system. The SE quantifies the degree of uncertainty involved in predicting the output of a probabilistic event. If one predicts the outcome of an event exactly before it happens, the probability will be a maximum value and as a result, the SE will be a minimum value. If one is absolutely able to predict the outcome of an event, the SE will be zero.

According to Zhong et al. (2009), the SE of any time-dependent signal can be defined as:

$$SE = -\sum_{i=1}^{N} p(x_i) \ln [p(x_i)] \quad (1)$$

where N is the length of the time series signal and $p(x_i)$ is the probability for appearance of every component in the signal.

Nedeltchev and Shaikh (2013) defined the probability as follows:

$$p(x_i) = \frac{x_i}{\sum_{i=1}^{N} x_i} \quad (2)$$

It is noteworthy that the SE profile increases monotonously and logarithmically and does not exhibit any local minimum at a particular superficial gas velocity. Fig. 1 shows that Eq. (1) in combination with Eq. (2) cannot be used for the flow regime identification in bubble columns.

Since the total sum of all points (60,000 in this case) is not a good choice (it yields extremely low probabilities) for the denominator, the summation was done for every 100 points and then, the probability for each point from this particular group was calculated. The same procedure was repeated for the next 100 points and so on. This approach gave more realistic probabilities. Based on them the modified SE was calculated. So, the main originality in the modification of the SE algorithm is the new definition of the probability, the calculation of SE in different signal parts and the introduction of a new dimensionless SE ratio.

The time series data characterized below were divided into 6 segments consisting of 10,000 points. The division of the time series into different segments is needed in order to identify the maximum and minimum SE values, SE_{max} and SE_{min}, respectively. In this work, it will be demonstrated that the dimensionless ratio SE_{min}/SE_{max} is a very reliable parameter for the flow regime identification in bubble columns.

The time series were also divided into two halves (each containing three segments). The SEs in the first three segments were summed and this gave the SE in the first half of the time series (SE_{FH}). Likewise, the SEs in the second three segments were summed and this gave the SE in the second half of the time series (SE_{SH}). It was found that the ratio SE_{FH}/SE_{SH} could be also used for flow regime identification.

The SE is measured in nats. The larger SE corresponds to more disorder in the system. This implies a more complex and chaotic nature resulting in turbulent motion of gas or liquid, intensive gas–liquid interactions, flow instabilities, etc.

3. Experimental setup

The local gas holdup (recorded in percentage) time series (60,000 points) were measured in a bubble column (0.15 m in ID) by means of conductivity wire-mesh sensor (see Fig. 2) consisting of a matrix-like arrangement of measuring points.

The bubble column was equipped with a perforated plate distributor (14 holes, Ø 4×10^{-3} m, open area (OA) = 1%) and operated with an air-deionized water system at ambient conditions. The clear liquid height was adjusted at 2.0 m. The wire-mesh sensor was installed at 1.3 m (in the fully developed region) above the gas distributor. Thirteen different superficial gas velocities U_G varying from 1.16×10^{-2} to 14.60×10^{-2} m/s with an increment of about 0.01 m/s have been investigated.

The wire-mesh sensor consisted of two electrode planes each with 24 stainless-steel wires of 0.2×10^{-3} m and 6.125×10^{-3} m lateral distance between the wires. The distance between the planes was 4.0×10^{-3} m (where the fluid resistance (or conductance) is measured) and the wires from different planes ran at right angles to each other. This arrangement gave 576 crossing points, thereof 452 inside the circular cross-section of the column. The matrix-like wire arrangement with the two perpendicular wire planes builds just virtual crossing points. Basically, the resistance (or conductance) in the gap of the artificial crossing is measured.

One plane of the electrodes acted as a transmitter, the other as a receiver. The transmitter electrodes were activated by a multiplexing circuit in a successive order and signals derived from the measured current at the receiver electrodes were recorded.

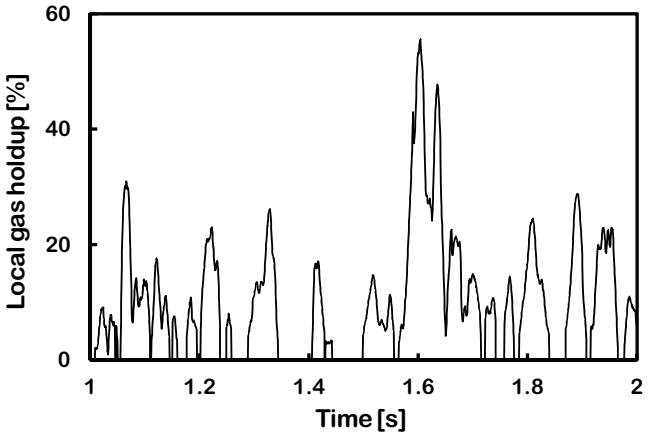

Fig. 3 – Typical local gas holdup fluctuations in the center of the cross-section of the bubble column at $U_G = 0.034$ m/s.

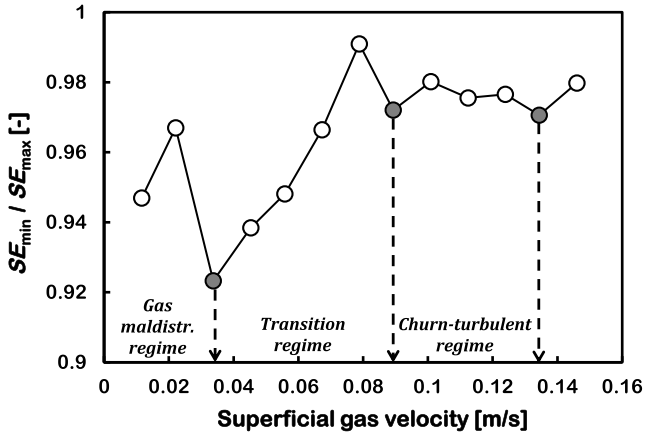

Fig. 4 – Dimensionless SE ratio as a function of U_G in the center (r/R = 0) of the column's cross-section.

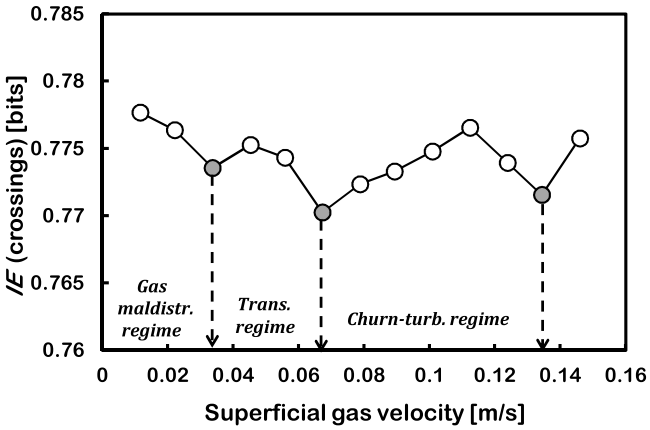

Fig. 5 – Information entropy extracted from the number of crossings as a function of U_G in the center (r/R = 0) of the column's cross-section.

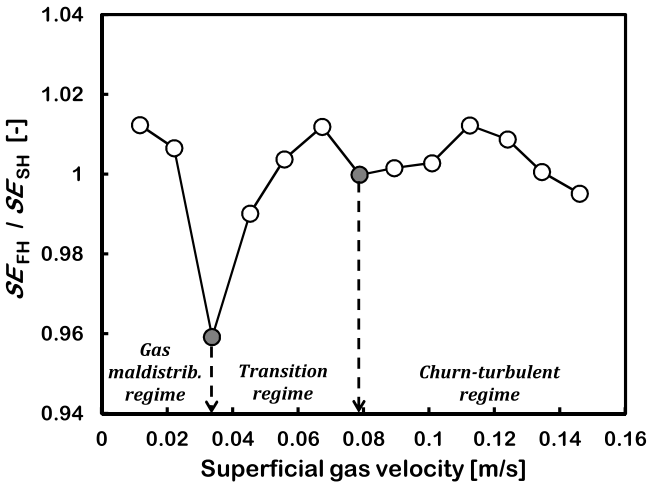

Fig. 6 – Ratio of the summed SE values in the first and second half of the time series as a function of U_G values in the center (r/R = 0) of the column's cross-section.

By applying an excitation signal to the transmitter wires one by one (multiplexing), the electrical current flowing towards the receiver wires is recorded fully in parallel by means of transimpedance amplifiers followed by analog to digital converters (ADC). This is carried out by the corresponding electronic circuitry and can be speeded up to 10,000 frames per second. For more details, the reader is referred to Prasser et al. (1998). The gas fraction in every individual crossing point is determined assuming a more or less linear relation between the measured signal in the crossing point and the local instantaneous gas holdup. The data therefore are normalized by measurement data from non-aerated column filled with water.

The local gas holdup time series were recorded at three different dimensionless radial (r/R) positions: 0.0 (core), 0.63 (inversion point of the axial liquid velocity) and 0.88 (annulus). Fig. 3 shows a typical signal in the core of the column at $U_G = 0.034$ m/s. It should be noted that the signal at each radial position contains some zero values (only liquid at this particular moment) which have been removed in order to apply the logarithmic function in Eq. (1).

The wire-mesh sensor is very suitable for studying the effect of the radial position on the main transition velocities. This goal cannot be achieved by a pressure transducer flush mounted with the wall. In addition, the time series measured by a pressure transducer are more susceptible to noise.

4. Results and discussion

4.1. *Flow regime identification at r/R = 0.00*

Fig. 4 shows that the dimensionless SE ratio in the column core (at r/R = 0.0) is capable of identifying the two main transition velocities U_{trans} and the end of the churn-turbulent flow regime. A well-pronounced minimum at $U_G = 0.034$ m/s distinguishes the end of the gas maldistribution regime and the beginning of the transition regime. The existence of the gas maldistribution regime has been documented by Nedeltchev et al. (2015). The second local minimum occurs at $U_G = 0.089$ m/s and marks the onset of the churn-turbulent flow regime. The upper boundary of the churn-turbulent flow regime is identifiable at $U_G = 0.134$ m/s. Most likely, beyond this critical U_G value follows the slug flow regime.

The extraction of the information entropy (see Fig. 5) from the number of crossings at r/R = 0 confirms that the end of the gas maldistribution regime occurs at $U_G = 0.034$ m/s and that the churn-turbulent regime ends at $U_G = 0.134$ m/s. Fig. 5 shows also that the churn-turbulent flow regime begins at $U_G = 0.067$ m/s.

Fig. 6 exhibits that in the center of the column's cross-section the ratio of the summed SEs from the first three segments of the time series divided by the summed SEs from the second three segments is also a reliable identifier of the

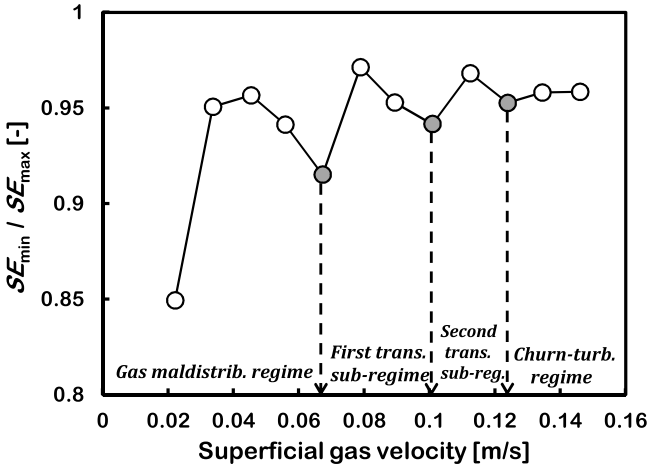

Fig. 7 – Dimensionless SE ratio as a function of superficial gas velocity at the inversion point (r/R = 0.63) of axial liquid velocity.

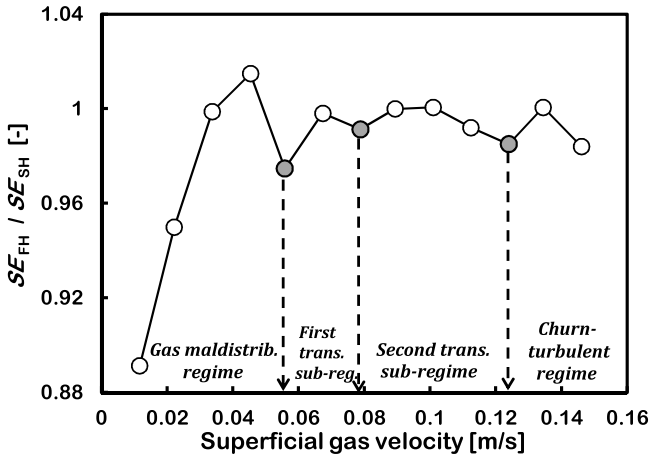

Fig. 8 – Ratio of the summed SE values in the first and second half of the time series as a function of U_G at the inversion point (r/R = 0.63) of axial liquid velocity.

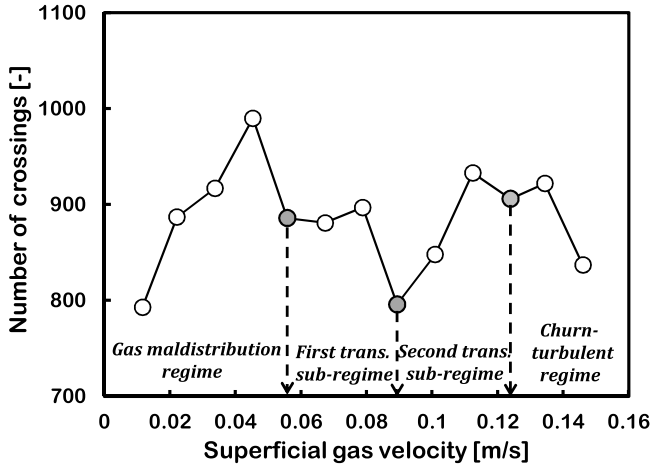

Fig. 9 – Number of crossings as a function of U_G at the inversion point (r/R = 0.63) of axial liquid velocity.

two main U_{trans} values. Two well-pronounced local minima occur at $U_G = 0.034$ m/s and $U_G = 0.079$ m/s and they identify the onsets of transition and churn-turbulent flow regimes, respectively.

A comparison between the results shown in Figs. 4–6 reveal that there is only a small uncertainty about the value of the second transition velocity. In all three figures, the first U_{trans} value occurs at $U_G = 0.034$ m/s. This experimental value is very close to the one (0.029 m/s) predicted for air-water system by the correlation of Reilly et al. (1994). Nedeltchev et al. (2015) reported that the first transition velocity occurs at 0.034 m/s when the cross-sectional average gas holdups are analyzed.

4.2. *Flow regime identification at r/R = 0.63*

Fig. 7 shows that the SE ratio at the inversion point (r/R = 0.63) of the axial liquid velocity at different U_G values is capable of identifying three transition velocities U_{trans}.

Wu and Al-Dahhan (2001) argue that the inversion point of the axial liquid velocity and the liquid circulation velocity in an air-water system occurs at a dimensionless radius of about 0.7. At $U_G = 0.067$ m/s, a well-pronounced local minimum distinguishes the end of the gas maldistribution regime. At $U_G = 0.101$ m/s a second local minimum occurs, which identifies the boundary between the first and the second transition sub-regime (Olmos et al., 2003a,b). Finally, at $U_G = 0.124$ m/s the dimensionless SE ratio identifies the onset of the churn-turbulent flow regime.

The delayed end of the gas maldistribution regime can be confirmed by the SE_{FH}/SE_{SH} ratio shown in Fig. 8. At $U_G = 0.056$ m/s a local minimum marks the end of the gas maldistribution regime. The boundary between both transition sub-regimes is successfully identified at $U_G = 0.079$ m/s. At $U_G = 0.124$ m/s, a local minimum distinguishes the onset of the churn-turbulent flow regime. A comparison between the results in Figs. 7 and 8 reveals that the first and second U_{trans} values identified by the SE_{FH}/SE_{SH} ratio occur somewhat earlier, whereas the third U_{trans} value is identified at the same U_G by both dimensionless SE ratios.

The surprisingly large range of stability of the gas maldistribution regime at r/R = 0.63 is confirmed by the values of the number of crossings of the mean as a function of U_G. Fig. 9 shows that the first well-pronounced local minimum occurs at $U_G = 0.056$ m/s, which marks the end of the gas maldistribution regime. The second U_{trans} value is identifiable at $U_G = 0.089$ m/s and this is the most clearly identifiable minimum in Fig. 9. The result based on the number of crossings implies that the churn-turbulent flow regime begins at $U_G = 0.124$ m/s.

The results shown in Figs. 7–9 demonstrate that the flow patterns around the inversion point involve the development of both first and second transition sub-regimes and their formation renders the flow structure much more complicated.

4.3. *Flow regime identification at r/R = 0.88*

Fig. 10 shows that the dimensionless ratio SE_{min}/SE_{max} close to the wall at the radial position r/R = 0.88 (annulus) is also capable of identifying the two main transition velocities U_{trans}. The first one is identifiable at $U_G = 0.045$ m/s on the basis of a local minimum. It distinguishes the onset of the transition flow regime. The second local minimum is located at 0.089 m/s and it distinguishes the second U_{trans} value, i.e. the beginning of the second transition sub-regime. The onset of the churn-turbulent flow regime is identifiable at $U_G = 0.124$ m/s. It seems that the upper boundary of the churn-turbulent regime can be identified by the dimensionless SE ratio only in the core of the bubble column.

The previous results of Nedeltchev et al. (2015) based on the information entropy extracted from the number of cross-

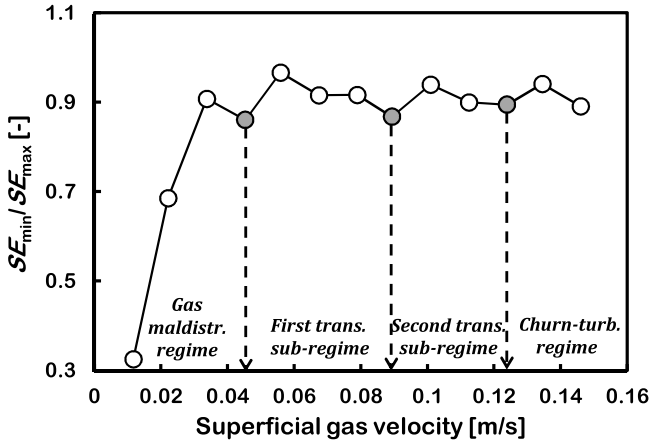

Fig. 10 – Dimensionless SE ratio as a function of U_G at a dimensionless radial position of 0.88.

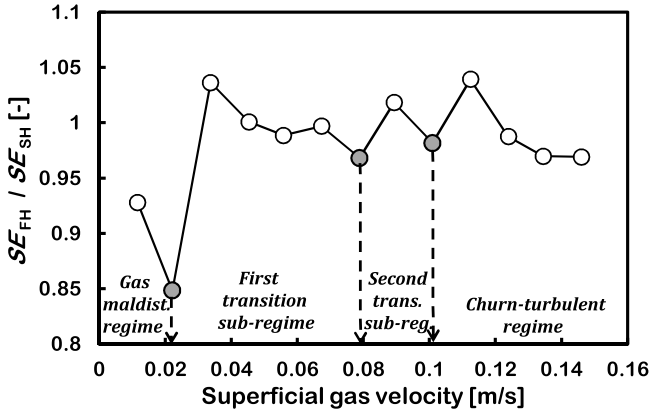

Fig. 11 – Ratio of the summed SE values in the first and second half of the time series as a function of U_G values at a dimensionless radial position of 0.88.

ings showed that at this radial position the first U_{trans} value occurs at 0.045 m/s, whereas the second U_{trans} value occurs at 0.112 m/s.

The SE_{FH}/SE_{SH} ratio in the annulus (see Fig. 11) identifies different U_{trans} values. Surprisingly, the first well-pronounced local minimum occurs at $U_G = 0.022$ m/s. The boundary between both transition sub-regimes is identifiable at $U_G = 0.079$ m/s. At $U_G = 0.101$ m/s begins the churn-turbulent flow regime.

The uncertainty about the location of the first transition velocity at the annulus can be resolved by means of the Kolmogorov entropy (KE). Fig. 12 shows that the first U_{trans} value occurs at 0.045 m/s, which confirms that this is the correct first transition velocity at $r/R = 0.88$. The boundary between both transition sub-regimes is identifiable (based on a well-pronounced local minimum) at $U_G = 0.101$ m/s. At $U_G = 0.124$ m/s begins the churn-turbulent flow regime.

5. Summary of the transition velocities in both core and annulus

The most important comparison is the one between the transition velocities in the core and annulus of the bubble column. Table 2 summarizes the results based on the SE_{min}/SE_{max} ratio. It is clear that both the transition and churn-turbulent flow regime begin earlier in the core of the column. This is due to the earlier start of bubble coalescence in the central region caused by the higher number of bubbles (and smaller distance between them) therein. The upper boundary of the churn-turbulent flow regime can be identified only in the core.

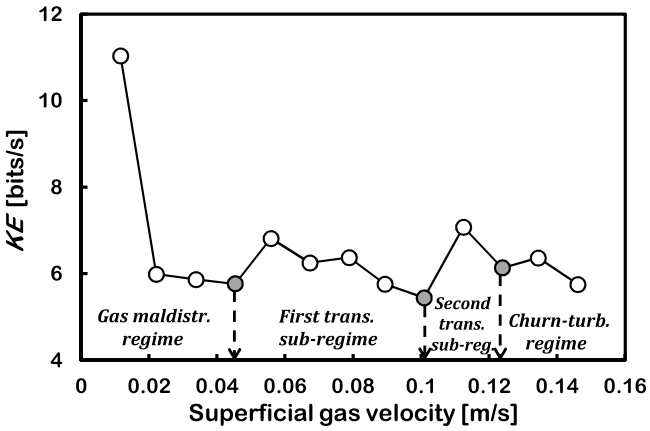

Fig. 12 – KE values (embedding dimension = 50, time delay = 1) as a function of U_G at a dimensionless radial position of 0.88.

Table 2 – Summary of the main transition velocities in both core and annulus of the column.

Type of transition	Core	Annulus
Onset of transition regime	$U_G = 0.034$ m/s	$U_G = 0.045$ m/s
Onset of churn-turbulent regime	$U_G = 0.089$ m/s	$U_G = 0.124$ m/s
End of churn-turbulent regime	$U_G = 0.134$ m/s	–

6. Conclusions

A new dimensionless ratio based on the modified Shannon entropy (SE) was defined and used for a successful identification of the main transition velocities in a bubble column (0.15 m in ID) operated with an air-water system at ambient conditions. The effect of the radial position on the transition velocities was investigated for the first time. It was found that the gas maldistribution regime ended earlier in the core of the column.

The new method identified most accurately (based on well-defined local minima) the flow regime boundaries when it was applied to time-dependent signals recorded in the core of the column. It was found that at the inversion point of the axial liquid velocity the end of the gas maldistribution regime was delayed, i.e. it shifted to higher superficial gas velocities. The churn-turbulent flow regime in the core occurred earlier than in the annulus. This fact is explainable with the earlier occurrence of bubble coalescence in the core of the column. Furthermore, it was possible to identify the upper boundary of the churn-turbulent flow regime in the core of the column.

A comparison between the ratio of the minimum SE over the maximum SE (SE_{min}/SE_{max}) and the ratio of the summed SEs in the first half of the time series divided by the summed SEs in the second half (SE_{FH}/SE_{SH}) was performed. Some differences in the transition velocities based on both parameters were distinguished.

Acknowledgments

The authors gratefully acknowledge the financial support of the European Research Council (ERC Starting Grant, Grant Agreement No. 307360). The financial support of the Helmholtz Association of German Research Centers within the

frame of the Initiative and Networking Fund is also acknowledged (No. ERC-0010).

References

Ajbar, A., Al-Masry, W., Ali, E., 2009. Prediction of flow regimes transitions in bubble columns using passive acoustic measurements. Chem. Eng. Process. 48, 101–110.

Anderson, J.L., Quinn, J.A., 1970. Bubble columns: flow transitions in the presence of trace contaminants. Chem. Eng. Sci. 25, 373–380.

Besagni, G., Inzoli, F., 2016. Comprehensive experimental investigation of counter-current bubble column hydrodynamics: holdup, flow regime transition, bubble size distributions and local flow properties. Chem. Eng. Sci. 146, 259–290.

Krishna, R., Ellenberger, J., 1996. Gas holdup in bubble column reactors operating in the churn-turbulent flow regime. AIChE J. 42, 2627–2634.

Kantarci, N., Borak, F., Ulgen, K.O., 2005. Bubble column reactors. Process Biochem. 40, 2263–2283.

Kikuchi, R., Yano, T., Tsutsumi, A., Yoshida, K., Puncochar, M., Drahoš, J., 1997. Diagnosis of chaotic dynamics of bubble motion in a bubble column. Chem. Eng. Sci. 52, 3741–3745.

Letzel, H.M., Schouten, J.C., Krishna, R., Van den Bleek, C.M., 1997. Characterization of regimes and regime transitions in bubble columns by chaos analysis of pressure signals. Chem. Eng. Sci. 52, 4447–4459.

Lin, T.-J., Tsuchiya, K., Fan, L.-S., 1999. On the measurements of regime transition in high-pressure bubble columns. Can. J. Chem. Eng. 77, 370–374.

Lin, T.-J., Juang, R.-C., Chen, Y.C., Chen, C.-C., 2001a. Predictions of flow transitions in a bubble column by chaotic time series analysis of pressure fluctuation signals. Chem. Eng. Sci. 56, 1057–1065.

Lin, T.-J., Juang, R.-C., Chen, C.-C., 2001b. Characterizations of flow regime transitions in a high-pressure bubble column by chaotic time-series analysis of pressure fluctuation signals. Chem. Eng. Sci. 56, 6241–6247.

Maruyama, T., Yoshida, S., Mizushina, T., 1981. The flow transition in a bubble column. J. Chem. Eng. Jpn. 14, 352–357.

Monahan, S.M., Vitankar, V.S., Fox, R.O., 2005. CFD predictions for flow-regime transitions in bubble columns. AIChE J. 51, 1897–1923.

Nedeltchev, S., Kumar, S.B., Duduković, M.P., 2003. Flow regime identification in a bubble column based on both Kolmogorov entropy and quality of mixedness derived from CARPT data. Can. J. Chem. Eng. 81, 367–374.

Nedeltchev, S., Shaikh, A., Al-Dahhan, M., 2006. Flow regime identification in a bubble column based on both statistical and chaotic parameters applied to computed tomography data. Chem. Eng. Technol. 29, 1054–1060.

Nedeltchev, S., Jordan, U., Lorenz, O., Schumpe, A., 2007. Identification of various transition velocities in a bubble column based on Kolmogorov entropy. Chem. Eng. Technol. 30, 534–539.

Nedeltchev, S., Shaikh, A., Al-Dahhan, M., 2011. Flow regime identification in a bubble column via nuclear gauge densitometry and chaos analysis. Chem. Eng. Technol. 34, 225–233.

Nedeltchev, S., Shaikh, A., 2013. A new method for identification of the main transition velocities in multiphase reactors based on information entropy theory. Chem. Eng. Sci. 100, 2–14.

Nedeltchev, S., 2015. New methods for flow regime identification in bubble columns and fluidized beds. Chem. Eng. Sci. 137, 436–446.

Nedeltchev, S., Hampel, U., Schubert, M., 2015. Experimental study on the radial distribution of the main transition velocities in bubble columns. WIT Trans. Eng. Sci. 89, 127–138.

Olmos, E., Gentric, C., Poncin, S., Midoux, N., 2003a. Description of flow regime transitions in bubble columns via laser Doppler anemometry signals processing. Chem. Eng. Sci. 58, 1731–1742.

Olmos, E., Gentric, C., Midoux, N., 2003b. Numerical description of flow regime transitions in bubble column reactors by a multiple gas phase model. Chem. Eng. Sci. 58, 2113–2121.

Pourtousi, M., Sahu, J.N., Ganesan, P., 2014. Effect of interfacial forces and turbulence models on predicting flow pattern inside the bubble column. Chem. Eng. Process.: Process Intensif. 75, 38–47.

Prasser, H.-M., Böttger, A., Zschau, J., 1998. A new electrode tomograph for gas-liquid flows. Flow Meas. Instrum. 9, 111–119.

Rabha, S., Schubert, M., Hampel, U., 2014. Regime transition in viscous and pseudo viscous systems: a comparative study. AIChE J. 60, 3079–3090.

Reilly, I.G., Scott, D.S., De Bruijn, T.G.W., MacIntyre, D., 1994. The role of gas phase momentum in determining gas holdup and hydrodynamic flow regimes in bubble column operations. Can. J. Chem. Eng. 72, 3–12.

Ribeiro Jr., C.P., Mewes, D., 2007. The influence of electrolytes on gas hold-up and regime transition in bubble columns. Chem. Eng. Sci. 62, 4501–4509.

Ruzicka, M.C., Drahoš, J., Fialova, M., Thomas, N.H., 2001a. Effect of bubble column dimensions on flow regime transition. Chem. Eng. Sci. 56, 6117–6124.

Ruzicka, M.C., Zahradnik, J., Drahoš, J., Thomas, N.H., 2001b. Homogeneous-heterogeneous regime transition in bubble columns. Chem. Eng. Sci. 56, 4609–4626.

Ruzicka, M.C., Drahoš, J., Mena, P.C., Teixeira, J.A., 2003. Effect of viscosity on homogeneous-heterogeneous flow regime transition in bubble columns. Chem. Eng. J. 96, 15–22.

Shah, Y.T., Kelkar, B.J., Godbole, S.P., Deckwer, W.-D., 1982. Design parameters estimations for bubble column reactors. AIChE J. 28, 353–379.

Shaikh, A., Al-Dahhan, M., 2007. A review on flow regime transition in bubble columns. Int. J. Chem. Reactor Eng. 5, Review R1.

Shiea, M., Mostoufi, N., Sotudeh-Gharebagh, R., 2013. Comprehensive study of regime transitions throughout a bubble column using a resistivity probe. Chem. Eng. Sci. 100, 15–22.

Vial, C., Camarasa, E., Poncin, S., Wild, G., Midoux, N., Bouillard, J., 2000. Study of the hydrodynamic behaviour in bubble columns and external loop airlift reactors through analysis of pressure fluctuations. Chem. Eng. Sci. 55, 2957–2973.

Vial, C., Lainé, R., Poncin, S., Midoux, N., Wild, G., 2001. Influence of gas distribution and regime transitions on liquid velocity and turbulence in a 3-D bubble column. Chem. Eng. Sci. 56, 1085–1093.

Wilkinson, P.M., Spek, A.P., Van Dierendonck, L.L., 1992. Design parameters estimation for scale up of high pressure bubble columns. AIChE J. 38, 544–554.

Wu, Y., Al-Dahhan, M.H., 2001. Prediction of axial liquid velocity profile in bubble columns. Chem. Eng. Sci. 56, 1127–1130.

Zahradnik, J., Fialova, M., Ruzicka, M.C., Drahoš, J., Kastanek, F., Thomas, N.H., 1997. Duality of gas-liquid flow regimes in bubble column reactors. Chem. Eng. Sci. 52, 3811–3826.

Zhong, W., Wang, X., Li, Q., Jin, B., Zhang, M., Xiao, R., Huang, Y., 2009. Analysis on chaotic nature of a pressurized spout-fluid bed by information theory based Shannon entropy. Can. J. Chem. Eng. 87, 220–227.